ACS OMEGA

http://pubs.acs.org/journal/acsodf

Article

# Cesium Removal from Nonexpandable Illite Clay by Chloride Salt Treatment

Sung-Wook Kim,* Ilgook Kim, Min Ku Jeon, Chan Woo Park, and In-Ho Yoon

Cite This: *ACS Omega* 2021, 6, 17923−17930

Read Online

ACCESS | Metrics & More | Article Recommendations

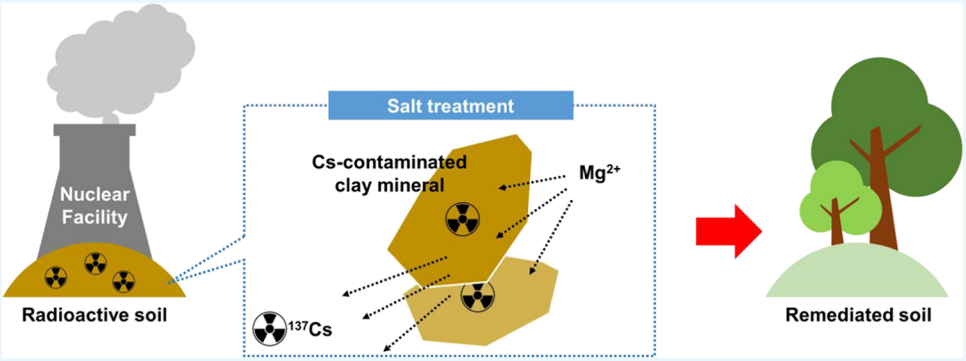


**ABSTRACT:** Extracting cesium (Cs) from nonexpandable illite clay is important in the remediation of radioactive Cs-contaminated soil. In this study, we investigated a chloride salt treatment technique for the removal of Cs from illite. Cs-loaded illite samples with initial Cs concentrations of 2430 and 690 ppm were treated using a $NaCl–MgCl_2–CaCl_2$ ternary salt system at 400−850 °C under ambient pressure to suppress Cs loss by vaporization. As a result of the treatment at 850 °C, wherein the salt was in a molten state, the Cs concentration was reduced by 99.5% (to 11.6 ppm) in the first sample and by 99.4% (to 3.86 ppm) in the second sample. Cs removal was achieved for these two samples even in a solid-state reaction at 400 °C, with reductions of 83.3% (407 ppm) and 73.3% (184 ppm), respectively. CsCl was formed by the reaction and remained stable in the salt. The incorporation of cations from the salt (mainly $Mg^{2+}$) to illite induced structural evolution forming an indialite phase to expel Cs from the clay samples.

## INTRODUCTION

Exposure to radioactivity, released from nuclear facilities during operation, accidents, and decommissioning, poses serious safety concerns for the public. Radioactive Cs (especially, $^{137}Cs$) significantly pollutes the environment owing to its easy spread in nature.[1−3] $^{137}Cs$ shows strong radioactivity ($\beta$ decays by itself and $\gamma$ decays from its metastable daughter nuclide, viz. $^{137m}Ba$) with a half-life of ∼30 years.[4] Since $Cs^+$ ions are highly soluble in water and behave similar to group I cations (e.g., $K^+$ ions) in living organisms, their intake is likely fatal.[5] It is well understood that $Cs^+$ ions have a strong affinity for clay minerals in soil;[6−9] thus, exposed Cs is expected to be incorporated into the soil. Vast amounts of soil have been contaminated by $^{137}Cs$ owing to nuclear power plant accidents at the Chernobyl and Fukushima Daiichi sites.[1−3] Plants grown in the contaminated soil may absorb $^{137}Cs$ and be consumed by humans, leading to critical health problems.

The soil washing method has been widely applied to decontaminate $^{137}Cs$-contaminated soil from nuclear sites.[10,11] In this method, the Cs sorption/desorption properties are strongly influenced by the type of clay minerals present in the soil, owing to the differences in their crystal structures and affinity for water molecules.[6] The removal of Cs from nonexpandable illite clay has been challenging because of the limited intercalation of water molecules into the interlayer and the strong binding of Cs in the interlayer and frayed edge sites.[7,8] Wendling et al. reported a 55% reduction in Cs from illite using an oxalate treatment.[7] In our recent studies, we achieved over 90% $^{137}Cs$ desorption in hydrobiotite, which is an expandable clay, using acid treatment under hydrothermal conditions, whereas we achieved ∼69% $^{137}Cs$ desorption in illite under identical experimental conditions.[8,9] Therefore, to increase the decontamination efficiency of actual contaminated soil composed of various clay minerals, a highly efficient technique should be developed for Cs removal from illite clay.

Received: March 22, 2021
Accepted: June 29, 2021
Published: July 9, 2021

Heat treatment that results in significant Cs removal by forming volatile species is an efficient decontamination approach.[12−16] In the presence of chloride salts, Cs in contaminated clay minerals can be transformed to CsCl, which is subsequently vaporized under low pressure upon heating.[14−16] Honda et al. reported that almost 100% Cs was removed from weathered biotite (WB) after NaCl−$CaCl_2$ treatment at 700 °C under vacuum conditions (~14 Pa).[15] This result was confirmed by X-ray fluorescence analysis.[16] The structural evolution of WB during heat treatment was revealed and thus the destabilization of Cs incorporated in the mineral was demonstrated.[16]

Complete vaporization and recovery of volatile Cs species are also challenging because of the difficulty in managing gas phases. These volatile species, with high boiling or sublimation temperature, often condense at unexpected low-temperature locations before they reach the capture system, thus disturbing the gas-phase motion and eventually blocking the gas exhaust line. Because the safe recovery of Cs released from clay minerals is important, it would be a more efficient strategy to maintain the removed Cs inside a condensed medium. CsCl has a relatively high boiling point (~1297 °C) and is thought to be hardly vaporized at ambient pressures at temperatures below 900 °C (Figure 1). Owing to the strong affinity of $Cs^+$ ions to $Cl^-$ ions, the potential Cs species released from the clay mineral (viz. Cs, $Cs_2O$, and CsOH) are expected to be converted to the chloride form, CsCl, in the presence of chloride salts (Table 1). Thus, the chloride salt treatment of Cs-contaminated soil within a mild temperature range and at ambient pressure would be an effective strategy for decontamination without Cs vaporization.

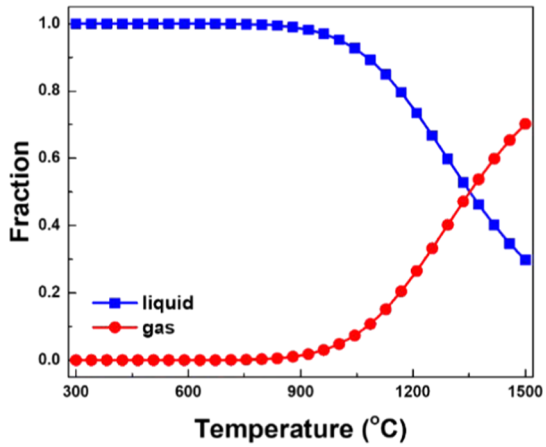


**Figure 1.** Equilibrium composition of CsCl in liquid and gas phases (at 1 atm) calculated from HSC Chemistry 9.

**Table 1. Thermodynamic Calculations for the Reactions of Cs, $Cs_2O$, and CsOH with Various Chloride Salts at 700 °C, Calculated from HSC Chemistry 9**

| reaction | $\Delta G$ (kJ) |
|---|---|
| Cs + NaCl = CsCl + Na | −28.660 |
| $Cs_2O$ + 2NaCl = 2CsCl + $Na_2O$ | −116.983 |
| CsOH + NaCl = CsCl + NaOH | −37.026 |
| 2Cs + $MgCl_2$ = 2CsCl + Mg | −231.457 |
| $Cs_2O$ + $MgCl_2$ = 2CsCl + MgO | −488.314 |
| 2CsOH + $MgCl_2$ = 2CsCl + $Mg(OH)_2$ | −290.235 |
| 2Cs + $CaCl_2$ = 2CsCl + Ca | −50.664 |
| $Cs_2O$ + $CaCl_2$ = 2CsCl + CaO | −362.091 |
| 2CsOH + $CaCl_2$ = 2CsCl + $Ca(OH)_2$ | −200.231 |

In this study, Cs decontamination properties were investigated using a ternary chloride salt system, NaCl−$MgCl_2$−$CaCl_2$. Lowering the reaction temperature is important for minimizing the formation of volatile species and reducing process costs. A ternary system with a low melting point (~420 °C at eutectic composition (NaCl/$MgCl_2$/$CaCl_2$ molar ratio = 53.44:31.61:14.95)) was introduced in this study.[17,18] $MgCl_2$ was chosen as an additive for the NaCl−$CaCl_2$ binary system used in the literature[15,16] to determine the effect of cation species ($Mg^{2+}$ vs $Ca^{2+}$) on the decontamination reaction. As shown in Table 1, the Gibbs free-energy change ($\Delta G$) of the $MgCl_2$ case is more negative than others, suggesting that the Mg addition would be beneficial for the Cs removal. Illite clay with a nominal composition of $K_{0.8-0.9}(Al,Mg,Fe)_2(Si,Al)_4O_{10}(OH)_2$, aged in an aqueous CsCl solution, was used as a surrogate for $^{137}$Cs-contaminated soil. The effect of temperature on Cs removal efficiency was surveyed over the temperature range of 400−850 °C, where the evaporation of CsCl was suppressed (Figure 1). The Cs release mechanism was tracked by combined inductively coupled plasma (ICP) spectroscopy, scanning electron microscopy (SEM) coupled with energy-dispersive X-ray spectroscopy (EDS), and X-ray diffraction (XRD) studies.

## RESULTS AND DISCUSSION

Figure 2a shows the brief flow diagram of the experiment. Two Cs-loaded illite samples (high Cs-loaded illite (HCIL) and low Cs-loaded illite (LCIL)) with different concentrations were prepared to investigate the decontamination properties. The Cs removal reaction was conducted inside an Ar-filled glovebox because the chloride salt is sensitive to moisture. Figure 2b shows the schematic diagram of an experimental setup for the chloride salt treatment. A vertically aligned reactor was connected to the glovebox for the heat treatment. After the salt treatment, the reaction products were rinsed with deionized water to recover the Cs-removed illite samples and the rinse water for analyses.

Table 2 confirms that the ternary chloride salt with the target composition was successfully prepared. The Cs-loaded illite samples were treated with this salt over the temperature range of 400−850 °C in an Ar-filled glovebox for the removal of Cs. Figure 3 shows the Cs concentrations of the illite samples before and after salt treatment. Clearly, the salt treatment is effective in separating Cs from the illite samples regardless of the initial Cs concentration, and that the removal efficiency was improved with increasing temperature. After the treatment at 850 °C, the Cs concentration was reduced to 11.6 and 3.86 ppm for the HCIL (2430 ppm) and LCIL (690 ppm) samples, respectively, indicating that more than 99% of Cs was removed by salt treatment. Notably, the Cs removal reaction occurred even at 400 °C, at which the salt is in the frozen state. This suggests that the chlorination of Cs in the illite samples forming CsCl can occur even by a solid-state reaction. Despite the relatively low conversion efficiency in the solid-state reaction (83.3% (407 ppm) and 73.3% (184 ppm) of Cs was removed from the HCIL and LCIL, respectively), the low-temperature process may be beneficial in terms of Cs recovery because evaporation of the Cs compounds should be difficult at this temperature, thus preventing gas-phase Cs loss. The decontamination factor (DF) is defined as the ratio of the Cs


https://doi.org/10.1021/acsomega.1c01516
ACS Omega 2021, 6, 17923−17930

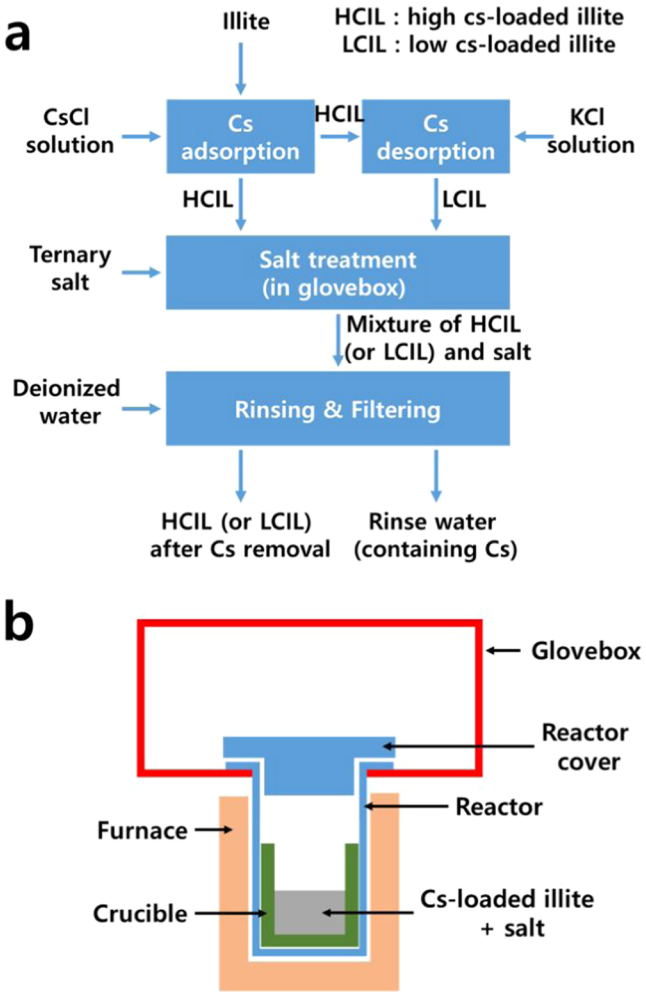


**Figure 2.** (a) Flow diagram of the experimental procedure and (b) schematic illustration of the Ar-filled glovebox system.

**Table 2. Composition Analysis of the NaCl−$MgCl_2$−$CaCl_2$ Ternary Chloride Salt**

| | | NaCl | $MgCl_2$ | $CaCl_2$ |
|---|---|---|---|---|
| input | total weight (g) | 20.82 | 20.06 | 11.06 |
| | cation weight (g) | 8.19 | 5.12 | 3.99 |
| | cation weight ratio | 2.05 | 1.28 | 1 |
| measured (ICP) | cation conc. (wt %) | 16.20 | 9.54 | 7.77 |
| | cation weight ratio | 2.08 | 1.23 | 1 |

concentration before and after the treatment. The DF values, simply calculated from the Cs concentration, were approximately 5.97/3.75, 10.08/7.23, 108.97/69.84, and 209.48/178.76 for HCIL/LCIL at 400, 550, 700, and 850 °C, respectively. There should be a trade-off between the removal efficiency and the process cost (temperature, time, and safety).

As described above, the safe and efficient recovery of Cs from illite samples is a major aim. The Cs concentration in the collected rinse water (500 mL) was tracked (using the HCIL sample at 850 °C) to identify the amount of Cs retained in the salt (Table 3). During the calculation, it was assumed that the residual salt was completely dissolved in the rinse water, and the change in the weight of the HCIL sample was negligible (0.999 g was recovered). Approximately 95% of the released Cs remained as dissolved ions in the rinse water, showing that Cs loss via vaporization was not substantial under this

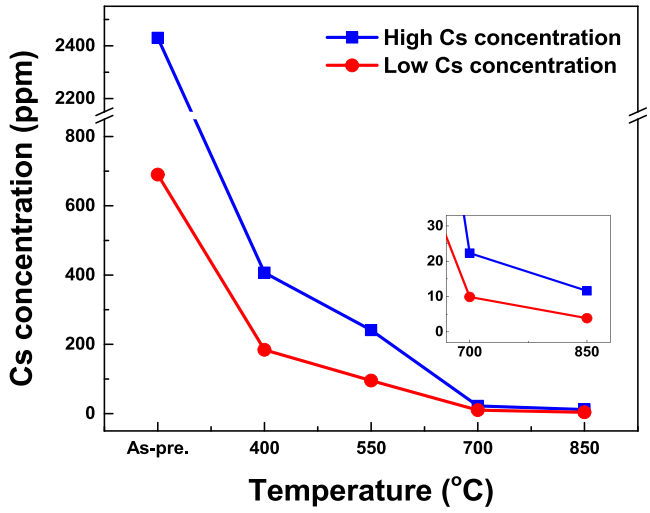


**Figure 3.** Cs concentration in illite samples before and after salt treatment at different reaction temperatures.

**Table 3. Cs Concentrations in the HCIL Sample and Rinse Water after Salt Treatment at 850 °C**

| content | amount |
|---|---|
| Cs concentration in the HCIL before the salt treatment | 2430 ppm |
| Cs concentration in the HCIL after the salt treatment | 11.6 ppm |
| Cs weight loss in the HCIL (in 1 g) | 2418.4 μg |
| Cs concentration in the rinse water | 4.59 ppm |
| Cs weight gain in the rinse water (in 500 mL) | 2295 μg |

condition, as expected (Figure 1). The rinse water should be treated as radioactive waste, and the dissolved $Cs^+$ ions in the water should be captured by subsequent wastewater treatment. For instance, Cs adsorbents with high selectivity to other alkali and alkaline-earth metal ions can be used to eliminate $Cs^+$ ions in rinse water.[19−21] Thereafter, the rinse water can be disposed of when its radioactivity meets regulations. Alternatively, the rinse water can be recycled after the appropriate salt separation treatment.

Simple heat treatment of the HCIL sample without the salt was conducted at 850 °C for comparison to identify the role of the chloride salt. The Cs concentration of the illite sample (unwashed state) was reduced to 222 ppm even after the simple heat treatment, suggesting the formation of volatile species, potentially Cs−O−H-based compounds.[22] This value is comparable to that of HCIL after salt treatment at 550 °C (241 ppm). Thus, it is evident that the presence of salt assists the release of Cs from the illite sample. Sufficient thermal energy supplied during simple heat treatment could form Cl-free volatile Cs compounds that vaporize from the illite sample. In contrast, the chloride salt treatment on the Cs contaminant tended to form CsCl that did not vaporize but remained in the salt at elevated temperatures (Table 3).

Results of detailed composition analyses with other elements for both the HCIL and LCIL samples treated at 850 °C are presented in Table 4. Si and Al, the major elements of general clay minerals, remained notably stable after salt treatment. Meanwhile, the concentrations of the minor elements, viz., Cs, Fe, and K, were significantly reduced after the reaction. The incorporation of Mg, Ca, and Na, which comprise the ternary salt, in the illite samples was identified. The concentration of Mg was considerably higher than those of the other elements,


https://doi.org/10.1021/acsomega.1c01516
ACS Omega 2021, 6, 17923−17930

**Table 4. Composition Analysis of Cs-Loaded Illite Samples before and after Salt Treatment at 850 °C**

| | HCIL (before) | HCIL (after) | LCIL (before) | LCIL (after) |
|---|---|---|---|---|
| Cs (ppm) | 2430 | 11.8 | 690 | 3.86 |
| Si (wt %) | 33.4 | 30.1 | 31.5 | 30.7 |
| Al (wt %) | 7.95 | 7.36 | 7.83 | 7.53 |
| Fe (wt %) | 1.84 | 0.14 | 1.75 | 0.124 |
| K (wt %) | 3.19 | 0.011 | 3.42 | 0.014 |
| Mg (wt %) | 0.243 | 9.60 | 0.224 | 9.17 |
| Ca (wt %) | | 0.124 | | 0.128 |
| Na (wt %) | | 0.157 | | 0.175 |

suggesting that $Mg^{2+}$ was the dominant cation incorporated into the illite samples.

The formation of a Mg-based phase was confirmed by XRD investigations, as shown in Figure 4. For both the HCIL and

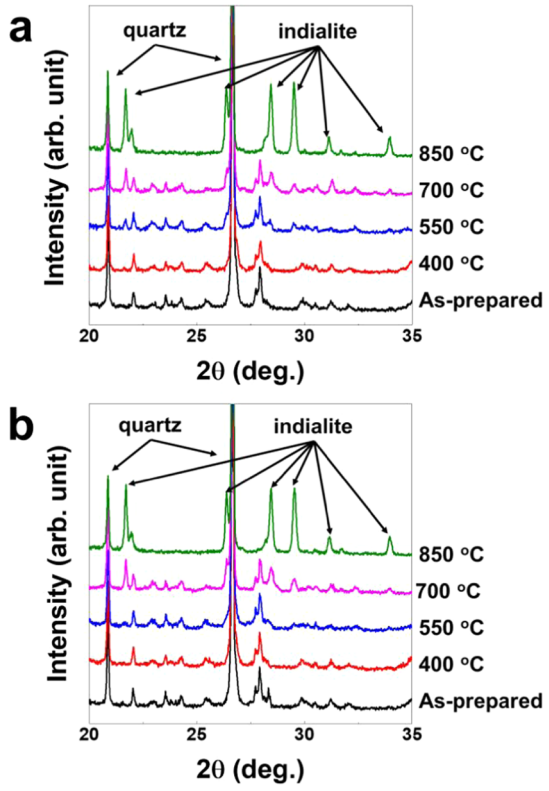


**Figure 4.** XRD patterns of (a) HCIL and (b) LCIL samples before and after salt treatment.

LCIL samples, the $Mg_2Al_4Si_5O_{18}$ phase (named indialite) appeared as temperature increased during salt treatment, demonstrating the impact of Mg incorporation on the structural evolution of the illite samples. Large diffraction peaks observed at approximately 20.9 and 26.7° correspond to $SiO_2$ (quartz) impurity, which was naturally present in the illite sample. Because of the high crystallinity of the quartz phase, clay samples could show the intense diffraction peaks even at a low $SiO_2$ content. Strong diffraction of the quartz phase was observed for the illite sample, whose purity is more than 90%.[23] The quartz peaks remained stable after the salt treatment, indicating the high stability of $SiO_2$ inside the chloride media. Meanwhile, the other diffraction peaks, corresponding to the clay phase, changed significantly. The indialite peaks (at approximately 21.71, 26.38, 28.44, 29.52, 31.72, and 33.96°) appeared above 550 °C, with the gradual disappearance of the original phase. This shows that sufficient thermal energy is required to induce the phase evolution to release Cs from the illite clay and the liquid-phase salt could be beneficial for the Cs removal reaction.

Figure 5 shows the SEM images and the corresponding elemental distributions (for Si and Mg, obtained by energy) of

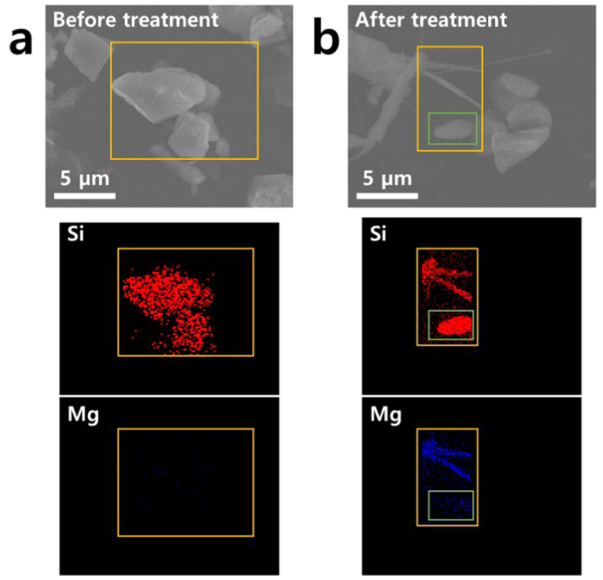


**Figure 5.** SEM-EDS images of the HCIL sample (a) before and (b) after salt treatment at 850 °C.

the HCIL sample before and after the treatment at 850 °C. The initial HCIL sample had a typical particle morphology. However, several microrods protruded out of the pristine particles during the reaction. The EDS maps (Figure 5b) show that Mg was highly concentrated in the microrods, although it was not observed clearly in the typical particle (green box), which was speculated to be the quartz impurity. This suggests that Mg incorporation led to morphological evolution.

Figure 6 shows the difference between the polyhedral arrangements of illite and indialite. Arrangements of Si/Al–$O_x$ polyhedral are quite different from each other (two-dimensional (2D) layered structure vs three-dimensional (3D) channel structure). For the chloride salt treatment technique, it is thought that the cations in the salt (especially, $Mg^{2+}$) can penetrate the illite structure considerably at elevated temperatures, as shown in Table 4. With an excessive amount of Mg in the illite clay, a Mg-based precipitate is formed (Figure 4) when sufficient heat energy for phase transformation is supplied. The phase evolution is the result of the search for the most stable state in a given condition. As the component of the mineral was changed, the original illite phase could not endure the stress induced by the incorporated cations in the layered framework and hence the energetically favored phase (indialite, in this case) should be evolved. Illite has strong Cs binding sites at the interlayer and frayed edge sites (edge portion of the layered structure) as described above.[7,8] With the structural evolution, the two-dimensional structure is completely destroyed and it is speculated that the stable Cs binding sites are eliminated. Consequently, destabilized $Cs^+$ ions were released from the clay minerals and subsequently combined with surrounding $Cl^-$ ions to form the chloride


https://doi.org/10.1021/acsomega.1c01516
ACS Omega 2021, 6, 17923−17930

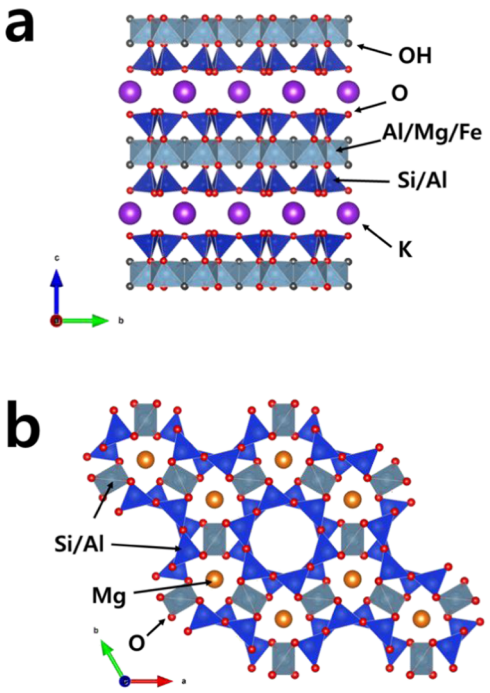


**Figure 6.** Crystal structures of (a) illite and (b) indialite.

phase (CsCl) in the salt. The simultaneous elimination of K and Fe (Table 4), which constitute the layered framework, also resulted in the destruction of the original illite structure. Mg is the key component of the indiaite phase, showing the impact of the Mg addition in the salt treatment.

Thus, the chloride salt treatment technique afforded improved Cs removal characteristics compared to the aqueous solution treatment for illite clay.[7,8] A recent study revealed that illite can be transformed into indialite in the presence of a Mg-based mineral (talc, $Mg_3Si_4O_{10}(OH)_2$) at high temperature (~1200 °C).[24] The reduced transformation temperature in our experiment might be due to high reactivity of the chloride salt compared to the stable clay mineral. In addition, a similar phase transformation via salt treatment was observed in a previous study by Honda et al.[16] They reported that WB was completely destroyed after NaCl−$CaCl_2$ treatment at 700 °C under 14 Pa to form a precipitate of an augite phase ($(Ca,Na)(Mg,Fe,Al)(Si,Al)_2O_6$) precipitate. It is considered that the type of original clay minerals and the salt composition strongly affected the phase of the precipitate. Further investigations to determine their relationship would be necessary to adopt this salt treatment technique for soil remediation.

The reason for the preferential penetration of $Mg^{2+}$ into the illite structure remains unclear. $\Delta G$ of the CsCl formation reactions shown in Table 1 can provide some information regarding this phenomenon. The $\Delta G$ values of Mg species in Table 1 are more negative than those of the Na/Ca analogues, suggesting that $Mg^{2+}$ is not energetically favored inside the chloride media in the presence of competing cation species. Additional thermodynamic calculations for the stability of the oxides of the clay components were performed in the coexistence of $MgCl_2$ (Table 5). $SiCl_4$, $AlCl_3$, and $FeCl_3$ were considered as gas phases because of their low boiling points (57.65, 180, and 315 °C for $SiCl_4$, $AlCl_3$, and $FeCl_3$, respectively). The calculations revealed that the chlorides of Cs and K are more stable than their oxides in the presence of

**Table 5. Thermodynamic Calculations for the Reactions of Various Oxides with $MgCl_2$ at 700 °C, Calculated from HSC Chemistry 9**

| reaction | $\Delta G$ (kJ) |
|---|---|
| $Cs_2O + MgCl_2 = 2CsCl + MgO$ | −488.314 |
| $K_2O + MgCl_2 = 2KCl + MgO$ | −472.286 |
| $SiO_2 + MgCl_2 = SiCl_4(g) + MgO$ | +179.138 |
| $Al_2O_3 + 3MgCl_2 = 2AlCl_3(g) + 3MgO$ | +251.128 |
| $Fe_2O_3 + 3MgCl_2 = 2FeCl_3(g) + 3MgO$ | +68.096 |
| $FeO + MgCl_2 = FeCl_2 + MgO$ | −30.939 |
| $Fe_3O_4 + 4FeCl_2 = FeCl_2 + 2FeCl_3(g) + 4MgO$ | +66.321 |

$MgCl_2$, while $SiO_2$ and $Al_2O_3$ are highly stable. The stability of Fe oxides is affected by the oxidation state of Fe. For instance, it is predicted that $Fe^{2+}$ is converted to $FeCl_2$ while $Fe^{3+}$ is not. The overall trend is in agreement with the experimental results in Table 4, suggesting the importance of thermodynamics in this process.

Because the illite samples (powder) and the salt formed complex mixtures when processed together in a crucible, the Cs-removed illite sample should be recovered by water treatment after cooling, as described earlier. This process requires a significant amount of time and resources. Heating and cooling each batch is considerably time consuming. In addition, this process needs larger quantities of salt and water than the target clay, which increases the process burden on their post-treatment.

Herein, we propose a simple technique to overcome these issues, as illustrated in Figure 7a. The illite samples were placed inside a porous crucible to ensure their contact with the molten salt during salt treatment. The porous crucible was then immersed in the molten salt for the Cs removal reaction. The illite samples were treated by simply inserting and extracting the porous crucible into and out of the molten salt; therefore, no repeated heating and cooling processes were required for each batch. Most of the Cs released was expected to accumulate inside the bulk salt. Only a small amount of residual salt containing Cs remained in the porous crucible; thus, the efforts required for the waste salt and water treatment can be significantly reduced. Furthermore, the salt/clay ratio can be increased, which should improve the Cs removal efficiency. The accumulated Cs in the bulk salt can be subsequently treated using the water treatment (dissolving and then capturing). Alternatively, dry salt purification techniques in the molten state[25,26] can be adopted for recycling the chloride salt and for minimizing wastewater generation.

To verify this concept, a porous MgO crucible was used in this study (Figure 7b). MgO is highly stable in the chloride media[27] and has been widely used as a structural material in the molten salt processes.[28,29] The HCIL-containing MgO crucible was stored inside the molten chloride salt at 700 °C and then recovered. The recovered MgO crucible remained stable after the experiment. The Cs removal behavior was investigated by ICP analysis, the results of which are shown in Table 6. The amount of Cs accumulated in the salt was almost identical to that in the pristine HCIL, showing that the decontamination reaction worked well even in the porous crucible, where salt-phase diffusion across the crucible wall was relatively slow. Although a porous ceramic crucible was used in this study to prevent the loss of the clay sample, adopting a meshed metal basket with a relevant opening size (smaller than


https://doi.org/10.1021/acsomega.1c01516
ACS Omega 2021, 6, 17923−17930

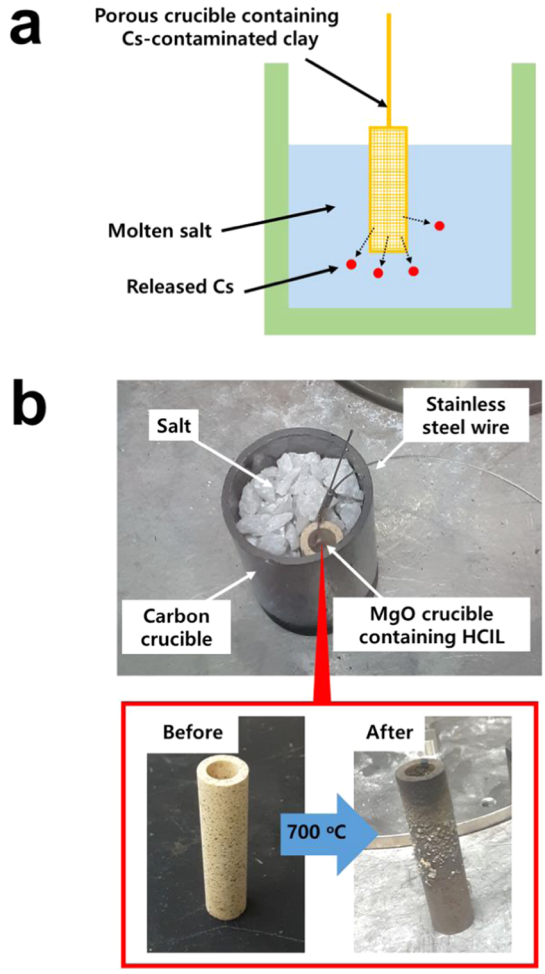


**Figure 7.** (a) Schematic of molten salt treatment using the porous crucible and (b) photographs of the experimental setup and the porous MgO crucible before and after treatment.

**Table 6. Cs Concentration in the HCIL and the Salt after Salt Treatment Using the Porous MgO Crucible at 700 °C**

| content | amount |
|---|---|
| Cs concentration in the HCIL before the salt treatment | 2430 ppm |
| HCIL loading weight | 3.11 g |
| Cs weight in the HCIL | 7557.3 $\mu$g |
| salt loading weight | 77.92 g |
| Cs concentration in the salt after treatment | 99.5 ppm |
| Cs weight gain in the salt | 7753.0 $\mu$g |

clay particles) would be a better approach in terms of salt diffusion and mechanical properties.

It has been reported that the radioactivity of $^{137}$Cs in the soils near the Fukushima site is in a range of $10^5$−$10^7$ Bq kg$^{-1}$,[30] which indicates that the $^{137}$Cs concentration in the actual contaminated soil is quite low (<ppb) compared to that under the experimental conditions employed in this study. Measurement of radioactivity is considered a promising method to determine the Cs concentration at a low contaminant level, and further investigations using the radioactive $^{137}$Cs are necessary to determine if this technique is still viable under extreme conditions.

## CONCLUSIONS

In this study, the decontamination of Cs in illite samples was investigated using a ternary chloride salt treatment (NaCl−$MgCl_2$−$CaCl_2$) over a temperature range of 400−850 °C. We conducted the experiment at ambient pressure to prevent the evaporation of Cs-containing volatile species. The Cs released from the illite samples was transformed into CsCl and remained stable in the salt. Higher temperatures led to higher Cs removal efficiencies, although Cs decontamination occurred even by the solid-state salt treatment (400 °C), in which the vaporization of Cs compounds was almost impossible. The structural evolution induced by cation incorporation (predominantly $Mg^{2+}$) released Cs contaminants from the illite samples. The proposed porous crucible technique can be used to improve the process properties. Because refractory Cs-contaminated illite clay can be treated by this technique, we are optimistic that this method could be a technical approach for the remediation of Cs-contaminated soil as well. Practical operation conditions can be set over a wide temperature range with a comprehensive consideration of Cs removal efficiency, Cs loss fraction, and process cost.

## MATERIALS AND METHODS

Illite clay samples were supplied by Yong−Koong Illite, Republic of Korea. Two Cs-loaded illite samples were prepared at high and low loading levels. For high Cs-loaded illite (HCIL), the pristine clay sample (20 g) was suspended in 200 mL of an aqueous solution containing 3 mM CsCl (Sigma-Aldrich, 99.9%) for 7 days at room temperature (~20−25 °C). Cs-loaded illite was collected by centrifugation and was air-dried. To prepare low Cs-loaded illite (LCIL), HCIL (10 g) was mixed with 1 L of an aqueous solution of 0.1 M KCl (Sigma-Aldrich, 99%) for 3 days at 25 °C for desorption of Cs and then recovered.

Near-eutectic compositions of NaCl (Sigma-Aldrich, 99%), $MgCl_2$ (Sigma-Aldrich, 98%), and $CaCl_2$ (Sigma-Aldrich, 97%) were mixed (Table 2) and then melted at 750 °C inside an Ar-filled glovebox (level of oxygen/moisture <50/1 ppm) to prepare the homogeneous ternary chloride salt. The temperature of the furnace was adjusted using a digital proportional integral derivative controller (UP35A, Yokogawa Electric Corporation). The heating rate was set to 5 °C min$^{-1}$ and a typical temperature variation at the target temperature was ±1 °C. No temperature control was employed during natural cooling. A subsequently frozen salt ingot was crushed to obtain the powder sample for the experiment.

Cs-loaded illite samples (1 g) were mixed with 3 g of the salt, and the mixtures were heated inside an $Al_2O_3$ crucible (diameter = 46 mm, thickness = 2.5 mm, height = 38 mm) at 400−850 °C for 12 h inside the Ar-filled glovebox. After cooling, the mixture was rinsed with 500 mL of deionized water and was vacuum-filtered. The filtered clay samples and rinse water were collected separately for analyses.

Another experiment was conducted with 3.11 g of the HCIL, which was placed inside a porous MgO crucible (diameter = 16.5 mm, thickness = 3.1 mm, height = 68 mm, porosity = ~25%, pore diameter = 6−8 $\mu$m) connected to a stainless-steel wire. The HCIL-containing MgO crucible was immersed into 77.92 g of the molten chloride salt (700 °C) inside a glassy carbon crucible (diameter = 56 mm, thickness = 3 mm, height = 82 mm). The MgO crucible was recovered using a stainless-


https://doi.org/10.1021/acsomega.1c01516
ACS Omega 2021, 6, 17923−17930

steel wire after immersion for 48 h. After treatment, the salt was collected via dipstick sampling.

ICP analyses with a mass spectrometer (iCAP 7400 duo, Thermo Scientific) and an atomic emission spectrometer (iCAP Qc, Thermo Scientific) were carried out to identify the contents of Cs and other elements (Si, Al, Fe, K, Mg, Ca, and Na). Particle shapes were observed using SEM (Hitachi, SU-8010), and the corresponding elemental distribution was obtained using EDS (Horiba, X-MAX) mapping. XRD (Bruker, D8 Advance) was used to determine the crystal structure.

## AUTHOR INFORMATION


### Corresponding Author

**Sung-Wook Kim** − *Decommissioning Technology Research Division, Korea Atomic Energy Research Institute, Daejeon 34057, Republic of Korea;* orcid.org/0000-0002-5537-4793; Phone: +82 42 868 8044; Email: swkim818@kaeri.re.kr; Fax: +82 42 868 2196

### Authors

**Ilgook Kim** − *Decommissioning Technology Research Division, Korea Atomic Energy Research Institute, Daejeon 34057, Republic of Korea*

**Min Ku Jeon** − *Decommissioning Technology Research Division, Korea Atomic Energy Research Institute, Daejeon 34057, Republic of Korea*

**Chan Woo Park** − *Decommissioning Technology Research Division, Korea Atomic Energy Research Institute, Daejeon 34057, Republic of Korea;* orcid.org/0000-0001-9805-512X

**In-Ho Yoon** − *Decommissioning Technology Research Division, Korea Atomic Energy Research Institute, Daejeon 34057, Republic of Korea;* orcid.org/0000-0001-8740-0573

Complete contact information is available at: https://pubs.acs.org/10.1021/acsomega.1c01516


### Author Contributions

K.S.-W. designed and performed the experiments. All authors contributed toward data analysis and discussion. This manuscript was written through the contributions of all authors. All authors have approved the final version of the manuscript.

### Notes

The authors declare no competing financial interest.

## ACKNOWLEDGMENTS

This work was supported by the National Research Foundation of Korea (NRF) grant funded by the Korea government, Ministry of Science and ICT (No. 2017M2A8A5015148).

## ABBREVIATIONS USED

WB, weathered biotite; ICP, inductively coupled plasma spectroscopy; SEM, scanning electron microscopy; EDS, energy-dispersive X-ray spectroscopy; XRD, X-ray diffraction; HCIL, high Cs-loaded illite; LCIL, low Cs-loaded illite

## REFERENCES


(1) Steinhause, G.; Brandl, A.; Johnson, T. E. Comparison of the Chernobyl and Fukushima nuclear accidents: a review of the environmental impacts. *Sci. Total Environ.* **2014**, *470−471*, 800−817.

(2) Wai, K.-M.; Krstic, D.; Nikezic, D.; Lin, T.-H.; Yu, P. K. N. External Cesium-137 doses to humans from soil influenced by the Fukushima and Chernobyl nuclear power plants accidents: A comparative study. *Sci. Rep.* **2020**, *10*, No. 7902.

(3) Matsuda, N.; Mikami, S.; Shimoura, S.; Takahashi, J.; Nakano, M.; Shimada, K.; Uno, K.; Hagiwara, S.; Saito, K. Depth profiles of radioactive cesium in soil using a scraper plate over a wide area surrounding the Fukushima Dai-ichi Nuclear Power Plant, Japan, Japan. *J. Environ. Radioact.* **2015**, *139*, 427−434.

(4) Waggoner, M. A. Radioactive decay of $Cs^{137}$. *Phys. Rev.* **1951**, *82*, 906−909.

(5) Avery, S. V. Caesium accumulation by microorganisms: uptake mechanisms, cation competition, compartmentalization and toxicity. *J. Ind. Microbiol.* **1995**, *14*, 76−84.

(6) Park, S. M.; Kim, J. G.; Kim, H. B.; Kim, Y. H.; Baek, K. Desorption technologies for remediation of cesium-contaminated soils: a short review. *Environ. Geochem. Health* **2020**, DOI: 10.1007/s10653-020-00667-3.

(7) Wendling, L. A.; Harsh, J. B.; Palmer, C. D.; Hamilton, M. A.; Flury, M. Cesium sorption to illite as affected by oxalate. *Clays Clay Miner.* **2004**, *52*, 375−381.

(8) Kim, S.-M.; Yoon, I.-H.; Kim, I.; Kim, J.-H.; Park, S.-J. Hydrothermal desorption of Cs with oxalic acid from hydrobiotite and wastewater treatment by chemical precipitation. *Energies* **2020**, *13*, 3284.

(9) Kim, S. M.; Yoon, I. H.; Kim, I. G.; Park, C. W.; Sihn, Y.; Kim, J. H.; Park, S. J. Cs desorption behavior during hydrothermal treatment of illite with oxalic acid. *Environ. Sci. Pollut. Res.* **2020**, *27*, 35580−35590.

(10) Liu, C.; Zachara, J. M.; Smith, S. C.; McKinley, J. P.; Ainsworth, C. C. Desorption kinetics of radiocesium from subsurface sediments at Hanford site, USA. *Geochim. Cosmochim. Acta* **2003**, *67*, 2893−2912.

(11) Kim, G.-N.; Choi, W.-K.; Jung, C.-H.; Moon, J.-K. Development of a washing system for soil contaminated with radionuclides around TRIGA reactors. *J. Ind. Eng. Chem.* **2007**, *13*, 406−413.

(12) Okumura, T.; Yamaguchi, N.; Dohi, T.; Iijima, K.; Kogure, T. Dissolution behaviour of radiocaesium-bearing microparticles released from the Fukushima nuclear plant. *Sci. Rep.* **2018**, *8*, No. 9707.

(13) Spalding, B. P. Volatilization of cesium-137 from soil with chloride amendments during heating and vitrification. *Environ. Sci. Technol.* **1994**, *28*, 1116−1123.

(14) Shimoyama, I.; Hirao, N.; Baba, Y.; Inzumi, T.; Okamoto, Y.; Yaita, T.; Suzuki, S. Low-pressure sublimation method for cesium decontamination of clay minerals. *Clay Sci.* **2014**, *18*, 71−77.

(15) Honda, M.; Okamoto, Y.; Shimoyama, I.; Shiwaku, H.; Suzuki, S.; Yaita, T. Mechanism of Cs removal from Fukushima weathered biotite by heat treatment with a NaCl-$CaCl_2$ mixed salt. *ACS Omega* **2017**, *2*, 721−727.

(16) Honda, M.; Shimoyama, I.; Kogure, T.; Baba, Y.; Suzuki, S.; Yaita, T. Proposed cesium-free mineralization method for soil decontamination: demonstration of cesium removal from weathered biotite. *ACS Omega* **2017**, *2*, 8678−8681.

(17) Du, L.; Tian, H.; Wang, W.; Ding, J.; Wei, X.; Song, M. Thermal stability of the eutectic composition in NaCl-$CaCl_2$-$MgCl_2$ ternary system used for thermal energy storage application. *Energy Procedia* **2017**, *105*, 4185−4191.

(18) Tian, H.; Wang, W.; Ding, J.; Wei, X.; Song, M.; Yang, J. Thermal conductivities and characteristics of ternary eutectic chloride/expanded graphite thermal energy storage composites. *Appl. Energy* **2015**, *148*, 87−92.

(19) Haas, P. A. A review of information on ferrocyanide solids for removal of cesium from solutions. *Sep. Sci. Technol.* **1993**, *28*, 2479−2506.

(20) Yang, H.-M.; Park, C. W.; Kim, I.; Yoon, I.-H. Hollow flower-like titanium ferrocyanide structure for highly efficient removal of radioactive cesium from water. *Chem. Eng. J.* **2020**, *392*, No. 123713.

(21) Kim, I.; Yang, H.-M.; Park, C. W.; Yoon, I.-H.; Seo, H.-K.; Kim, E.-K.; Ryu, B.-G. Removal of radioactive cesium from an aqueous

solution via bioaccumulation by microalgae and magnetic separation. *Sci. Rep.* **2019**, *9*, No. 10149.
(22) Roki, F. Z.; Chatillon, C.; Ohnet, M. N.; Jacquemain, D. Thermodynamic study of the CsOH(s,l) vaporization by high temperature mass spectrometry. *J. Chem. Themodyn.* **2008**, *40*, 401−416.
(23) Marsh, A.; Andrew, H.; Pascaline, P.; Mark, E.; Pete, W. Alkali activation behavior of un-calcined montmorillonite and illite clay minerals. *Appl. Clay Sci.* **2018**, *166*, 250−261.
(24) Wattanasiriwech, S.; Wattanasiriwech, D. Roles of talc-illite on phase transformation, vitrification, and physical properties of a triaxial porcelain body. *J. Ceram. Process. Res.* **2019**, *20*, 643−648.
(25) Versey, J. R.; Phongikaroon, S.; Simpson, M. F. Separation of CsCl from LiCl-CsCl molten salt by cold finger melt crystallization. *Nucl. Eng. Technol.* **2014**, *46*, 395−406.
(26) Choi, J.-H.; Lee, K.-R.; Kang, H.-W.; Park, H.-S. Reactive-crystallization method for purification of LiCl salt waste. *J. Radioanal. Nucl. Chem.* **2020**, *325*, 485−492.
(27) Hur, J.-M.; Kim, I.-S.; Lee, W.-K.; Cho, S.-H.; Seo, C.-S.; Park, S.-W. A study on the stability of MgO in a LiCl-$Li_2O$ molten salt system. *J. Ind. Eng. Chem.* **2004**, *10*, 442−444.
(28) Burak, A.; Chamberlain, J.; Simpson, M. F. $Li_2O$ entrainment during $UO_2$ reduction in molten LiCl-$Li_2O$: Part II. Effect of cathodic reduction mechanism. *J. Electrochem. Soc.* **2020**, *167*, No. 166513.
(29) Nikolaev, A.; Suzdaltsev, A.; Pavlenko, O.; Zaikov, Y.; Kurennykh, Y.; Vykhodets, V. Reduction of $ZrO_2$ during SNF pyrochemical reprocessing. *J. Electrochem. Soc.* **2021**, *168*, No. 036506.
(30) Kaneko, M.; Iwata, H.; Shiotsu, H.; Masaki, S.; Kawamoto, Y.; Yamasaki, S.; Nakamatsu, Y.; Imoto, J.; Furuki, G.; Ochiai, A.; Nanba, K.; Ohnuki, T.; Ewing, R. C.; Utsunomiya, S. Radioactive Cs in the severely contaminated soils near the Fukushima Daiichi nuclear power plant. *Front. Energy Res.* **2015**, *3*, No. 37.


https://doi.org/10.1021/acsomega.1c01516
*ACS Omega* 2021, 6, 17923−17930